Accurate phenology analyses require bud traits and energy budgets

Marc Peaucelle, Josep Peñuelas, Hans Verbeeck

Accurate phenology analyses require bud traits and energy budgets

Authors: Marc Peaucelle[1,2*], Josep Peñuelas[3,4], Hans Verbeeck[2]

Affiliations :
[1] INRAE, Université de Bordeaux, UMR 1391 ISPA, 33140 Villenave-d'Ornon, France
[2] Computational and Applied Vegetation Ecology - CAVElab, Department of Environment, Faculty of Bioscience Engineering, Ghent University, Gent, Belgium
[3] CSIC, Global Ecology Unit CREAF-CSIC-UAB, Bellaterra, 08193 Barcelona, Catalonia, Spain
[4] CREAF, Cerdanyola del Vallès, 08193 Barcelona, Catalonia, Spain

*Correspondence to: marc.peaucelle@inrae.fr

e-mail addresses: marc.peaucelle@inrae.fr, josep.penuelas@uab.cat, hans.verbeeck@ugent.be

Keywords: plant phenology, budburst, temperature, light, energy budget, modelling, climate warming

Spring phenology is mainly driven by temperature in extratropical ecosystems. Recent evidence highlighted the key role of micrometeorology and bud temperature on delaying or advancing leaf unfolding. Yet, phenology studies, either using ground-based or remote sensing observations, always substitute plant tissue temperature by air temperature. In fact, temperatures differ substantially between plant tissues and the air because plants absorb and lose energy. Here, we build on recent observations and well-established energy balance theories to discuss how solar radiation, wind, and bud traits might affect our interpretation of spring phenology sensitivity to warming. We show that air temperature might be an imprecise and biased predictor of bud temperature. Better characterizing the plants phenological response to warming will require new observations of bud traits and temperature for accurately quantifying their energy budget. Since consistent micrometeorology datasets are still scarce, new approaches coupling energy budget modelling and plant traits could help improving phenology analyses across scales.

Introduction

Plant phenology, the study of the timing of life-cycle events, drives several ecosystem functions, such as plant productivity and biomass, but also local and global climates by affecting biogeochemical and biogeophysical processes, such as carbon storage and energy fluxes[1,2], and the abundance and diversity of local flora and fauna, such as pollinators and herbivores[3,4]. Understanding the environmental controls and responses of plant phenology to climate change is thus essential for several sectors, e.g. agriculture, forestry and gardening[5], but also for conservation[6] and public health[7] (e.g. allergies).

It is now largely assumed that bud-break is induced by warming air temperature during spring[8] in temperate and boreal regions, and this is the reason why phenology assessments mainly rely on critical air temperature sums preceding leaf unfolding, often referred to as the Growing Degree Day concept. Climatic warming has strongly shifted phenophases in the Northern Hemisphere in recent decades[1,9–11]. Rising temperatures have lengthened the annual growth cycle by advancing leaf unfolding in spring and delaying leaf fall in autumn[12], albeit with variations among species[13] and regions[14]. Recent evidence, though, suggests that the sensitivity of spring phenology to warming is decreasing in northern forests[15] and that the rate of change in plant productivity does not match that of air temperature[16]. Indeed, plant phenology may be acclimated to long-term biogeographical constraints[17–19] and may be co-limited by several other factors, such as light[20], water[21–23] and nutrients[24]. These observations suggests that warming does not have the same effect everywhere[25], which has increased interest in other environmental drivers in recent decades, especially illustrated by multiple debates about the specific role of light (and photoperiodism) in spring phenology[20,26–33].

How light affects spring phenology remains an open question. Most commonly, its effect is considered via photoperiod, often referred to as daylength. The daylength hypothesis implies that the quality and/or quantity of light is somehow directly sensed by plants through biochemical mechanisms. Some recent studies suggest that the spectral composition of light can indeed influence foliar phenology[34,35]. Light also plays a key role in regulating phytohormones, but the underlying mechanisms remain unknown[32] and clearly require more investigation. More sporadically, the effect of light has been treated as the sum of insolation over a specific period[36], for which plants need a specific quotum for a phenological event to occur. The quantity and quality of light depend on plant location, which is the main reason why a response to daylength has often been proposed as a safety mechanism against frost at high latitudes and elevations. Only 35% of the woody species in the Northern Hemisphere, however, depend on daylength as a direct signal for leaf-out[20], and these species are mainly at mid- to low latitudes.

Light effect on spring phenology is still being debated. Recent studies nonetheless suggest a complex interaction between temperature and light. Daytime and nighttime temperatures during winter

and spring have an asymmetrical effect on leaf unfolding[37–41], with a greater weight of temperature during the day[38,42,43]. Whether or not plants are able to sense light, radiation has a physical impact on plants: it affects the temperatures of their tissues. Since temperature has been shown to be sensed at the bud level[44,45], omitting the physical effect of radiation introduces large biases into the interpretation of spring phenological responses based on air temperature.

In their recent study, Vitasse et al. highlighted the strong phenological effect of bud albedo and light exposure, explaining shifts in the budburst date reaching up to 12 days[44], and revealing an important role of microclimatic variation on phenology. Indeed, bud temperature (T_{bud}) depends on its energy balance[46]. During the day, plant tissues absorb both shortwave (SW, visible and near-infrared) and longwave (LW, infrared) radiation from the sky but also radiation emitted and reflected by the surrounding environment (vegetation, soil) (Fig. 1a). Only a fraction (α, absorptivity) of SW radiation will be absorbed depending on bud traits such as color, coating, shape and size (Fig. 1b), while most LW radiation will be absorbed by buds. According to the Stefan-Boltzmann law, buds lose energy via LW radiation emission, while they absorb LW radiation emitted from surrounding objects. Finally, a part of their energy is lost by conduction and mostly by convection[47,48] (e.g. due to wind) while leaves lose an important part of their energy via transpiration. T_{bud} increases when energy gains exceed losses (Fig. 2a) and vice-versa. T_{bud} can thus be lower than air temperatures (T_{air}) on clear nights[47] or because of wind. On the other hand, T_{bud} can be significantly higher than T_{air} during the day. The link between T_{bud} and energy balance has been known for more than 30 years [46,47]. Since then, all major studies linking temperature and photoperiod to phenological changes, however, have not accounted for the true temperature of plant organs.

What can we expect if we account for micrometeorology and bud temperature in phenological studies? Unfortunately, the lack of *in situ* observations for bud temperature does not allow to answer directly this question. As part of the reflection, we thus applied existing well-established energy balance approaches[46,47,49] to explore the potential variability in temperature of an isolated bud. This situation is well representative of the conditions encountered by sun-exposed buds of a tree, and especially of deciduous species (i.e. with no or minimum shading). As commonly applied in 'big-leaf" models where an entire canopy is represented by a single 'big' leaf, discussing the microclimate effect on an isolated bud will help us to explore the variability in phenology we can expect at different spatiotemporal scales and between species.

Results

Non-linear response of plant tissue temperature to microclimate

As a first example, we looked at the variability in T_{bud} estimated from its energy balance and site meteorological observations for an European Beech forest[52]. On average, T_{bud} is expected to be higher than T_{air} during the preseason (~1°C in our example; Fig. 2b). Day and night T_{bud} are higher or lower than T_{air} by several degrees. The temperature of buds thus strongly depends on the diurnal radiative cycle and the spectral composition of the light (SW/LW radiation), echoing the observed asymmetrical effect of diurnal temperatures on leaf unfolding[38,42,43]. Applied on four other sites, this approach leads to similar results despite differences in T_{bud} profiles induced by differences in radiation along a latitudinal gradient (Fig. 3). Spring phenology does not only respond to average preseason temperature, but mainly to the accumulated effect of temperature and its dynamics. It is often assumed that chilling and forcing temperature required for budburst are only effective over specific windows, generally between 0 and 5 °C and over 5°C, respectively. Daily bud temperature variability might thus be the most important factor influencing leaf unfolding, not necessarily its average temperature. We could expect that the difference in extremum temperature sensed by buds over the preceding months (ΔT_{min} and ΔT_{max}, Fig. 2b) will inevitably affect the apparent forcing and chilling requirement for leaf unfolding.

Accounting for the energy budget of buds for six common species across Europe (Extended Fig. 1) we also expect a stronger interannual variability in T_{bud} than T_{air}, as well as different temporal evolutions over the last decades (Fig. 4). In our example, buds are expected to warm faster or slower than air depending on location and species, with 13 % and 7 % of the sites exhibiting an increase and a decrease in ΔT over 1990-2015, respectively. These trends represent idealized sun-exposed conditions without site or species-specific calibration. Still, we observe that the heterogeneity in ΔT evolution results from a complex and non-linear response to the amount of absorbed radiation and convection processes (Extended Fig. 2). Because leaf unfolding is earlier in 2015 than in 1990, the average amount of absorbed radiation during the preseason slightly decreased over this period, while most of the interannual variability in ΔT is driven by conduction and convection (i.e. wind). The difference in air-bud temperature and their non-linear and non-proportional relationship suggests that our current interpretation of the apparent bud sensitivity to warming needs to account for the temperature sensed by the plant.

Response to warming relies on organ traits and microclimate

We illustrated the role of bud energy balance through an idealized and constant representation of buds and their environment for all sites and species. Larger spatial and temporal variations are expected

due to the effect of topography, ground albedo (e.g. snow, understory), differences in bud traits (Fig. 1b) and micrometeorological conditions[53] that will affect plant tissues energy balance. By affecting the amount of radiation reaching the buds (Fig. 1a), varying ground albedo from 0.1 (~wet bare soil) to 0.9 (~snow) leads to a doubling in preseason ΔT (Fig. 5). Since ground albedo strongly varies in space and over the preseason (e.g. snow), we can expect substantial differences in the phenological signal at the regional scale induced by radiation, as already observed from leaf unfolding observations[17].

Different bud colors or coating will also affect solar absorption of specific wavelengths, while shape and size will modify convection processes and the amount of intercepted radiation (Fig. 6), and hence, bud temperature. For example, Common Ash (*Fraxinus excelsior*) has black buds while sycamore (*Acer pseudoplatanus*) has green buds and mountain ash (*Sorbus aucuparia*) have dense white trichomes (i.e. hairs) on their surfaces. In our example, a difference in solar absorptivity of 0.3 leads to a doubling in ΔT (Fig. 2a, Fig. 3a). The differences in bud traits can thus partly account for the observed interspecific differences in heat requirement and apparent sensitivity to temperature. This suggests that the phenological response of plants to warming might be more species-specific than we thought, which should be accounted for in large scale studies.

Discussion

Despite its central role at the organ level[53,54], micrometeorology is rarely accounted for in phenology studies because rarely measured, or simply because it is impossible to account for its effect such as in remote sensing analysis or terrestrial biosphere modelling. Instead, phenology studies, either local or regional, often use meteorological and climate datasets with hourly to daily time resolutions. The use of a steady state energy balance is easily justified under such conditions since thermal time constants of tree buds varies between a few seconds to about ten minutes [55]. Accounting for average preseason radiation and wind conditions might better explain the observed variability in plant phenology than air temperature alone. Here, we only explored spring T_{bud} variability in the case of sun-exposed buds with no shading. Accounting for the potential protecting effect of leaves or needles in evergreen species might substantially attenuate the effects of radiation and wind on intra- and bottom-canopy buds. The concomitant use of high-resolution microclimate data and transient energy budget models will be needed to quantify such effects.

Drivers of phenological events and light are virtually impossible to separate, because daylength and radiation are strongly correlated with the time of year. Accounting for organ energy balances is thus promising for separating the environmental drivers of phenology using a single approach and potentially for reconciliating the differences observed in the field. Applying existing modelling approaches in the

context of sun-exposed buds suggested that air temperature might be an imprecise and biased predictor of bud temperature and more importantly of its variability over the months preceding leaf unfolding, which might introduce biases in the analysis of chilling and forcing requirement for budburst. However, we also showed that bud temperature results from a complex combination of several biotic and abiotic factors, and under certain conditions air temperature might remain a good proxy for bud temperature. The examples we have presented open new avenues to investigate and refine our interpretation of plant phenological acclimation to warming that were solely based on air temperature. For example, changes in spring radiation regimes over the last decades[56,57] have been hypothesized to increase discrepancies between standard air temperature and bud temperature[44], which is in line with the energy budget theory described in this perspective. However, current observations do not allow such reassessment. Bud traits and *in situ* temperature observations are scarcely described in the literature. New experiments and observations are clearly needed for accurately quantifying the traits and energy budget of buds. Existing studies have mostly focused on leaves, but other organs should also be investigated. Key traits that will need to be measured to assess the interspecific variability of phenology include organ traits influencing solar absorptivity and heat storage, but organ temperatures (i.e. using thermocouples) concomitant with micrometeorological variables will also need to be directly measured. With the assumption that bud transpiration is negligible, their energy budget is simpler than for leaves. Properly calibrated, accounting for bud energy balance could improve the accuracy of phenological models that are still unable to predict the spatiotemporal variability of plant dynamics with satisfactory accuracy[58]. Such approach could not only improve spatiotemporal assessments of phenology (e.g. based on ground-based and remote sensing observations), but also provide new insights into ecosystem functioning such as the influence of global warming synchrony between flowers and insects, or between plant functions and climate (e.g. growth and soil moisture, signaling, etc.).

Finally, we stress that energy balance affects the temperature extrema sensed by plants (Fig. 2b). The lengthening of the growing season in recent decades has also been associated with an increase in environmental risks. For example, earlier leaf unfolding exposes plants to late frost[59–61] in spring, potentially resulting in dramatic impacts on agriculture[62–64] and forestry[65,66]. The use of energy balances to study and better predict these environmental risks can provide novel insights into the responses of plants to extreme temperatures and offer more robust predictive tools, which are essential for developing adaptation measures and reducing the ecological and economic impacts. Temperature of plant organs and their dynamics are still overlooked in both environmental studies and modeling exercises[67]. Energy balance thus plays a key role, not only for plant phenology but also for all other processes since plant

198 tissue temperature will govern key mechanisms such as photosynthesis and respiration and the general
199 functioning of the plant.
200

Online methods

Description of the bud energy budget model

We implemented a simplified energy budget model for buds based on Landsberg et al. [47], Hamer[46], as well as equations from Jones[50] and Muir[49]. We refer to Supplementary Table S1 for parameter values and units. Our implementation follows the 'big-leaf' concept for which the whole canopy is simplified by a single representative organ, here an isolated bud in a deciduous canopy.

For an isolated bud, the amount of absorbed incoming radiation (R_{abs}) is balanced by the thermal infrared radiation loss (LW_{bud}) and the energy lost by conduction and convection, generally called the sensible heat flux (H). The thermal time constant of buds is less than a minute[55], meaning that bud temperature responds quite rapidly to local changes. Because most phenology studies use meteorological data from local stations or gridded datasets, here we simulate bud temperature by considering that the energy balance is close to equilibrium at a time scale of a few minutes, which is consistent with temporal resolution of meteorological observations from FLUXNET sites (30 min) and CRU-JRA[68] (6 h) and the thermal time constant of buds ranging from a few seconds to a few minutes[55]:

$$R_{abs} = LW_{bud} + H \quad (1)$$

As we consider the energy budget of the whole, two-sided bud, and not the projected area, the amount of absorbed energy by buds is the sum of incoming shortwave (SW, visible and near-infrared) and longwave (LW, infrared) radiations from the sky and the ground:

$$R_{abs} = \alpha_{sw}(1 + r)SW + \alpha_{lw}(LW_{sky} + LW_{gnd}) \quad (2)$$

where α_{sw} is the bud absorptivity to SW; r is the fraction of SW reflected by the ground and α_{lw} is the bud absorptivity to LW, which is here defined as the average of LW coming from the atmosphere LW_{sky} and coming from the ground LW_{gnd}.

LW emitted by surrounding objects such as branches were considered equal to LW emitted from the ground and the sky. We set α_{lw} to 0.97, which corresponds to the average absorptivity for wood and leaves [50,69,70]. Since no data were available in the literature, we tested two different values of α_{sw}, 0.5 and 0.8, corresponding to values commonly used for broadleaves and needleleaves, respectively. We set r to 0.2, which corresponds to a reasonable value for the fraction of SW reflected by grasses. Of course, r will strongly vary according to the albedo of the ground (e.g. understory/grass, forest litter, snow, etc.), which was simplified here for our perspective paper.

LW_{gnd} was computed from ground temperature following the Stefan-Boltzmann equation:

$$LW_{gnd} = \sigma \varepsilon T_{gnd}^4 \quad (3)$$

where σ is the Stefan-Boltzmann constant and ε is the bud emissivity to longwave radiations (which is equal to α_{lw} since plant material tends to behave like a black body in the IR spectrum[50]).

This is important to keep in mind that ground temperature will strongly depend on soil type, vegetation and snow cover but also soil humidity.

Buds lose thermal infrared radiation proportionally to their temperature as:

$$LW_{bud} = 2\sigma \varepsilon T_{bud}^4 \quad (4)$$

where σ is the Stefan-Boltzmann constant and ε is bud emissivity to longwave radiations. As for the absorbed radiation, radiations are emitted on both sides of the bud (i.e. toward the sky and the ground).

Finally, the sensible heat flux depends on the air to bud temperature gradient and is formulated as in Muir[49]:

$$H = 2\rho_a c_p g_b (T_{bud} - T_{air}) \quad (5)$$

where ρ_a is the density of the air; c_p is the specific heat capacity of air at constant pressure and g_b is the boundary-layer conductance to heat.

$$\rho_a = \frac{P}{R_a} T_a \frac{(1 + q_a)}{\left(1 + \frac{R_w}{R_a} q_a\right)} \quad (6)$$

where P is the atmospheric pressure, R_a and R_w are the specific gas constant for dry air and water vapor, respectively, T_a is the temperature of the air and q_a is the specific humidity of the air.

$$g_b = \frac{D_h Nu}{d} \quad (7)$$

where Nu is the Nusselt number, D_h is the diffusion coefficient of heat in air and d is the bud diameter.

$$D_h = D_{h,0} \left(\frac{T}{273.15}\right)^{eT} \frac{101.3246}{P} \quad (8)$$

D_h is function of temperature and pressure, $D_{h,0}$ corresponds to D_h at 0°C and eT is the temperature dependence of diffusion.

The Nusselt number is estimated as a mixed convection such as:

$$Nu^{3.5} = Nu_{forced}^{3.5} + Nu_{free}^{3.5} \quad (9)$$

with

$$Nu_{forced} = e + aRe^{b} \quad (10)$$

and

$$Nu_{free} = f + cGr^{d} \quad (11)$$

Re and *Gr* are the Reynolds and Grashof numbers, respectively; *a, b, c* and *d* are constants that are dependent of the flow regime.

In our example, we simplified bud's shape as a spherical object with a diameter of 5 mm to computes the boundary-layer conductance to heat. Please refers to Hamer[46] for a detailed discussion of this assumption, as well as empirical formulations for the convective heat transfer of apple buds. Condition for laminar and turbulent flows, as well as constants *a, b, c* and *d* for a spherical object, as well as for objects of various forms, can be found in Monteith and Unsworth[71]. This is a simplification to keep in mind when calculating convection processes for different species with various bud shapes and for which the close proximity of branches can modify the flow regime. Also, the evolution of turbulence and sensible heat transfer from the bud to the canopy scale (associated with aerodynamic conductance in addition to bud boundary layer one) was not considered here, and was implicitly accounted for in the form of air temperature.

In addition, we performed two simulations varying ground albedo from 0.1 (~wet bare soil) to 0.9 (~snow) and bud diameter from 5 to 13 mm (Fig. 5 and 6)

Note that a proper calibration of species and site properties (e.g. albedo) is needed to use this model for predictions. Here, we used already existing models and assumptions for the only purpose of exploring the expected variability in bud temperature with environmental conditions and for an isolated object representative of apical buds in a tree. Model development and validation was not intended here and will require *in situ* observations of bud traits and temperature data.

The bud energy model simulates bud temperature in idealized conditions and at equilibrium, without distinction between species and sites and several simplifications as described above.

Still, we describe in the two following sections how to account for bud energy storage as well as latent heat from wet buds in rainy conditions. Both implementations were tested without significant changes in the results and the corresponding code is also implemented and available in the model.

Accounting for energy storage

We applied the same approach accounting for the thermal time constant of buds, which is dependent on bud traits and its associated thermal resistance. Following Jones[50], the change in bud temperature with time (*t in s*) follows:

$$\frac{dT}{dt} = S/\rho^* c_p^* l^* \quad (12)$$

with S the energy stored by the bud in W m^{-2}, ρ^* and c_p^* are the density in kg m^{-3} and the specific heat capacity in J kg^{-1} K^{-1} of the bud and l^* is the volume to area ratio, corresponding to *d/4* for a cylinder and *d/6* for a sphere, with d the bud diameter in m.

Between two equilibrium states, this first-order differential equation gives the following bud temperature:

$$T_{bud}(t) = T_{eq}(t) - [T_{eq}(t) - T_{bud}(t_{-1})]\exp(-t/\tau) \quad (13)$$

with T_{eq} the bud temperature at equilibrium and τ the thermal time constant in s (see eq. 9.8, eq. 9.9 and eq. 9.10, p. 227 in Jones[50]) which is function of the conditions in the boundary layer[55,72] (i.e. bud traits and wind):

$$\tau = \frac{\rho^* c_p^* l^*}{hA} \quad (13)$$

with A the wetted area in m² and h the heat transfer coefficient in W m^{-2} K^{-1} following:

$$h = \frac{Nu\lambda_a}{d} \quad (13)$$

with λ_a the thermal conductivity of air in W m^{-2} K^{-1}.

Michaletz & Johnson[55] estimated average values of τ ranging from 8 to 30 s for 12 different species with an average value of 13 s. The effect of energy storage is thus negligible with >30 min resolution meteorological data. Using high resolution micrometeorological observations should lead to better results by accounting for rapidly changing radiation load with clouds, wind speed, bud inclination etc.

Accounting for wet conditions

We implemented an option to account for latent heat in the model in order to simulate the cooling effect of evaporation when buds are wet because of the rain or dew conditions.

The maximum water density (d_w) on buds depends on bud orientation, size and hydrophilicity. Since no data were found in the literature regarding water interception from buds, we defined the maximum interception reservoir based on leaf data. In the literature, d_w for leaves varies between 0.05 and 0.2 mm[73]. We thus arbitrary set d_w for buds to 0.15 mm. Varying d_w from 0 to 0.2 mm (kg m^{-2}) did not change the results.

The maximum surface water content Wc_{max} (in kg) intercepted by a bud was thus calculated as:

$$Wc_{max} = d_w \times S_b \quad (14)$$

With S_b the surface area of the bud in m².

Surface water content (Wc) was estimated at each time step as the balance between water inputs from rain and dew and water outputs from evaporation. First, water coming from the rain of the previous time step is added to current Wc as:

$$Wc = min(Wc_{max}, (Wc + rain \times S_b)) \quad (15)$$

Then, latent heat energy dissipated by evaporation or accumulated from condensing dew (E) was calculated based on Wc following Gerlein-Safdi et al.[74]:

$$E = \begin{cases} \lambda_v(T_{bud}) \dfrac{dWc}{dt}, if \ \dfrac{dWc}{dt} > 0 \\ \lambda_c(T_{bud}) \dfrac{dWc}{dt}, if \ \dfrac{dWc}{dt} < 0 \end{cases} \quad (16)$$

with the latent heat of condensation λ_c (in J kg^{-1}) being equal of the latent heat of vaporization λ_v. The surface water content balance can be written as:

$$\frac{dWc}{dt} = 0.622 \, S_b \, \rho_a \, g_h \left[\frac{e_c(T_{air}) - e_{sat}(T_{bud})}{P} \right] \quad (17)$$

with g_h the conductance of the boundary layer to water vapor in m s^{-1}, e_c the vapor pressure in Pa and e_{sat} the saturating vapor pressure in Pa.

Here, water does not modify the diffusion coefficient of heat in air D_h.

Accounting for latent heat in the energy budget did not change the results.

Datasets and analysis

Half-hourly forcing meteorological and soil temperature data (Fig. 2, 3, 5 and 6) were downloaded from the FLUXNET2015 dataset at https://fluxnet.fluxdata.org/data/fluxnet2015-dataset/. Historical climate data from CRU-JRA[68] at a spatial resolution of 0.25° and at a temporal resolution of 6 h (Fig. 4 and Extended Fig. 2) were downloaded at https://catalogue.ceda.ac.uk/uuid/13f3635174794bb98cf8ac4b0ee8f4ed. Soil temperature data at 0.25° were downloaded from ECMWF-ERA5[75] reanalysis with the 'KrigR' package[76].

In situ leaf unfolding data (Fig. 4 and Extended Fig. 2) for Common alder (*Alnus glutinosa*), horse chestnut (*Aesculus hippocastanum*), silver birch (*Betula pendula*), European beech (*Fagus sylvatica*), European ash (*Fraxinus excelsior*) and pedunculate oak (*Quercus robur*) were downloaded from the Pan European Phenology network (http://www.pep725.com/). Phenological observations followed the Biologische Bundesanstalt, Bundessortenamt und Chemische Industrie (BBCH) code, with leaf unfolding corresponding to BBCH = 11. Only sites with more than 20 years of observation over the 1990-2015 period were used, corresponding to 5050 sites*species in total, covering 1059 sites (Extended Fig. 1). Analysis and figures were generated with the R v3.5.1 software[77].

Data availability

FLUXNET2015 data are available at https://fluxnet.fluxdata.org/data/fluxnet2015-dataset/

CRU-JRA data are available at https://catalogue.ceda.ac.uk/uuid/13f3635174794bb98cf8ac4b0ee8f4ed

ERA5 soil temperature data are available at https://cds.climate.copernicus.eu/cdsapp#!/dataset/reanalysis-era5-land

PEP725 phenology data are available at http://www.pep725.eu/

Code availability

The R code of the model of energy budgets and data sets used to generate the figures and analysis of this manuscript are available from Github at https://github.com/mpeaucelle/Tbud

A version of the git repository is archived on Zenodo at https://zenodo.org/record/5897267 corresponding to tag v.2.0.

Acknowledgments

The authors would like to acknowledge Dr. Chris Muir and Dr. Renée Marchin Prokopavicius for their constructive feedbacks on our work. M.P. would like to acknowledge the financial support from the Fonds Wetenschappelijk Onderzoek (FWO; grant no. G018319N) and the H2020 Marie Skłodowska-Curie Actions (LEAF-2-TBM grant no. 891369). J.P. would like to acknowledge the financial support from the European Research Council Synergy grant ERC-SyG-2013-610028 IMBALANCE-P, the Spanish Government grant PID2019-110521GB-I00, the Fundación Ramon Areces grant ELEMENTAL-CLIMATE, and the Catalan Government grant SGR 2017-1005. H.V. acknowledges the support from the European Research Council Starting Grant 637643 TREECLIMBERS.

Author Contributions Statement

M.P. designed the study, performed the analysis and wrote the first version of the manuscript. J.P. and H.V. substantially contributed to the interpretation of the results and the revisions of the manuscript. All authors read and approved the final manuscript.

Competing Interests Statement

The authors declare no competing interests

Figures

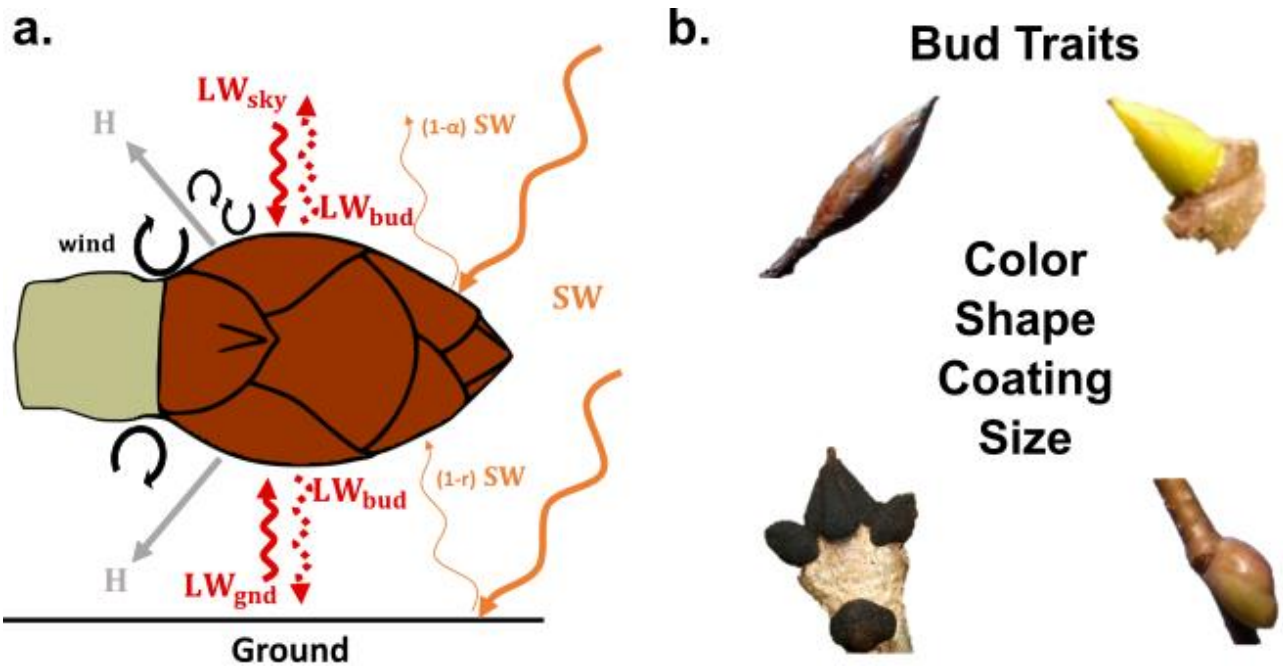

Figure 1 | Energy budget of buds and bud traits. a. Buds lose energy through convection and conduction (H). Buds absorb incoming shortwave (visible and near-infrared, SW) and longwave (infrared, LW) radiation from the sky (LW_{sky}) and the surrounding environment (here simplified as LW radiation from the ground, LW_{gnd}). Buds emit LW radiation as a function of their temperature (LW_{bud}). Only a fraction (α) of SW radiation is absorbed by buds, depending on the properties of their surfaces. Buds also absorb a small fraction of SW reflected from the ground (1-r). **b.** Illustration of bud traits influencing solar absorptivity, heat conduction and convection processes, and hence, bud temperature.

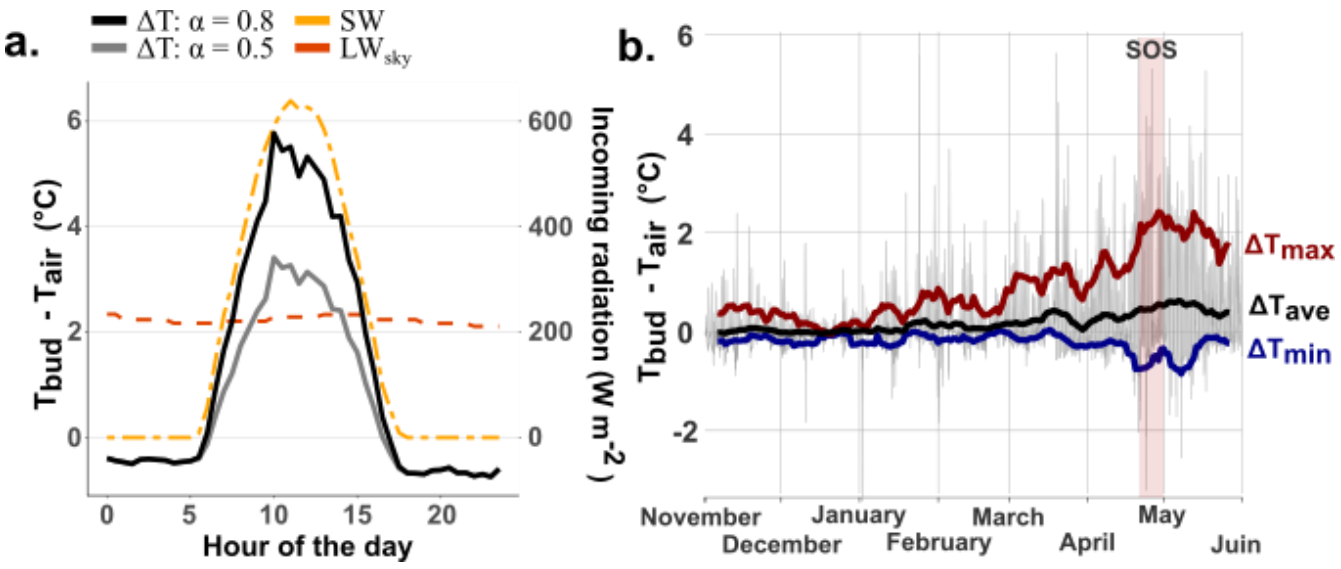

Figure 2 | Simulated differences in temperature between buds and the air (ΔT) from energy balance. a. Daily variation in ΔT for an exposed bud and a typical day in April for two solar absorptivities: α=0.5 (typical for broad leaves[50]) and α=0.8 (typical for needle leaves[50]). SW and LW_{sky} correspond to the amount of incoming shortwave and longwave radiation from the sky. **b** Example of ΔT simulated under idealized conditions (e.g. exposed buds in a deciduous canopy) using meteorological observations for winter and spring collected at the Hainich FLUXNET site[51] (temperate deciduous forest). The grey lines represent half-hourly differences in temperature simulated using an energy-budget model. The blue, black and red curves represent the 10-d rolling mean of the minimal (ΔT_{min}), average (ΔT_{ave}) and maximal (ΔT_{max}) temperature differences, respectively. Approximative Start Of growing Season (SOS) is illustrated by the light red region.

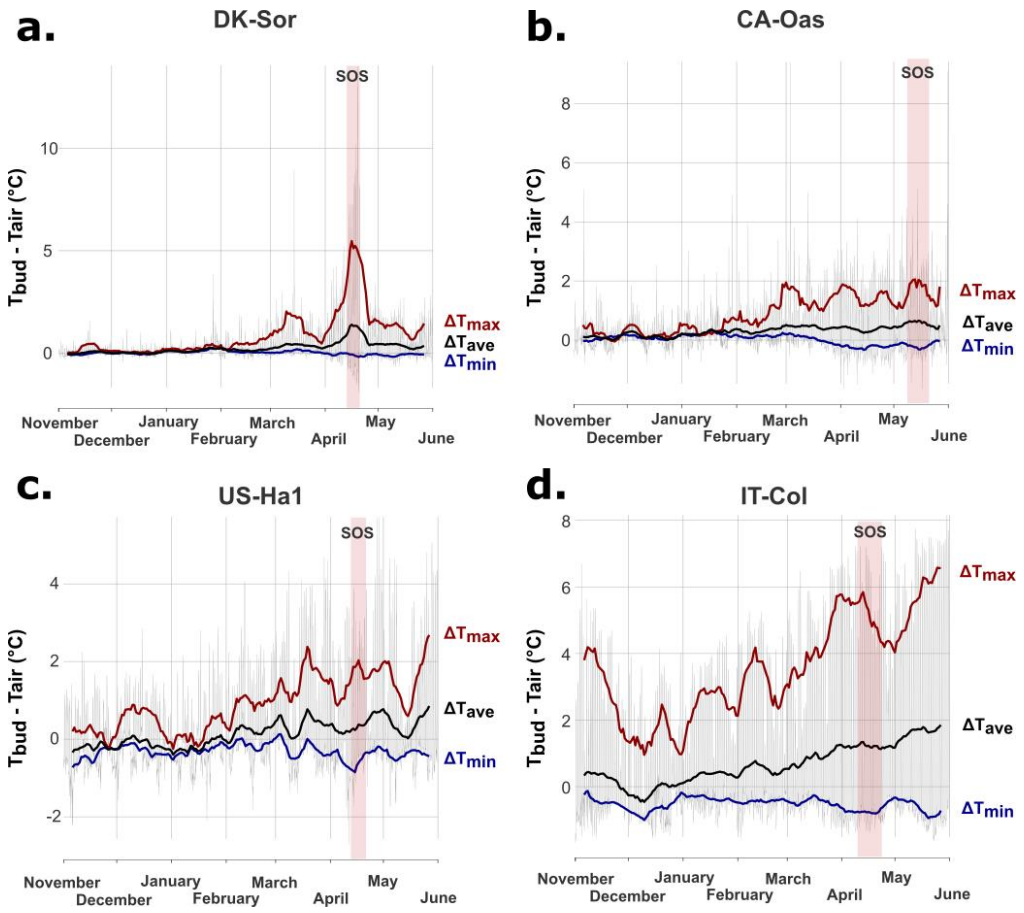

Figure 3 | Spatial variability in bud temperature. Temperature difference (ΔT in °C) between buds and air simulated for four different FLUXNET sites during the year 1998: DK-Sor (Deciduous Broadleaf Forest; 55.48 °N, 11.64 °E), CA-Oas (DBF; 53.63° N, 106.20° W), US-Ha1 (DBF; 42.53 °N, 72.17 °W) and IT-Col (DBF; 41.85°N, 13.59°E). The grey lines represent half-hourly differences in temperature simulated using the energy-budget model. The blue, black and red curves represent the 10-d rolling mean of the minimal (ΔT_{min}), average (ΔT_{ave}) and maximal (ΔT_{max}) temperature differences, respectively. Approximative Start Of growing Season (SOS) based on fluxes is illustrated by the light red region. Note that these simulations represent idealized conditions and use the same parameterization without distinction between sites and species.

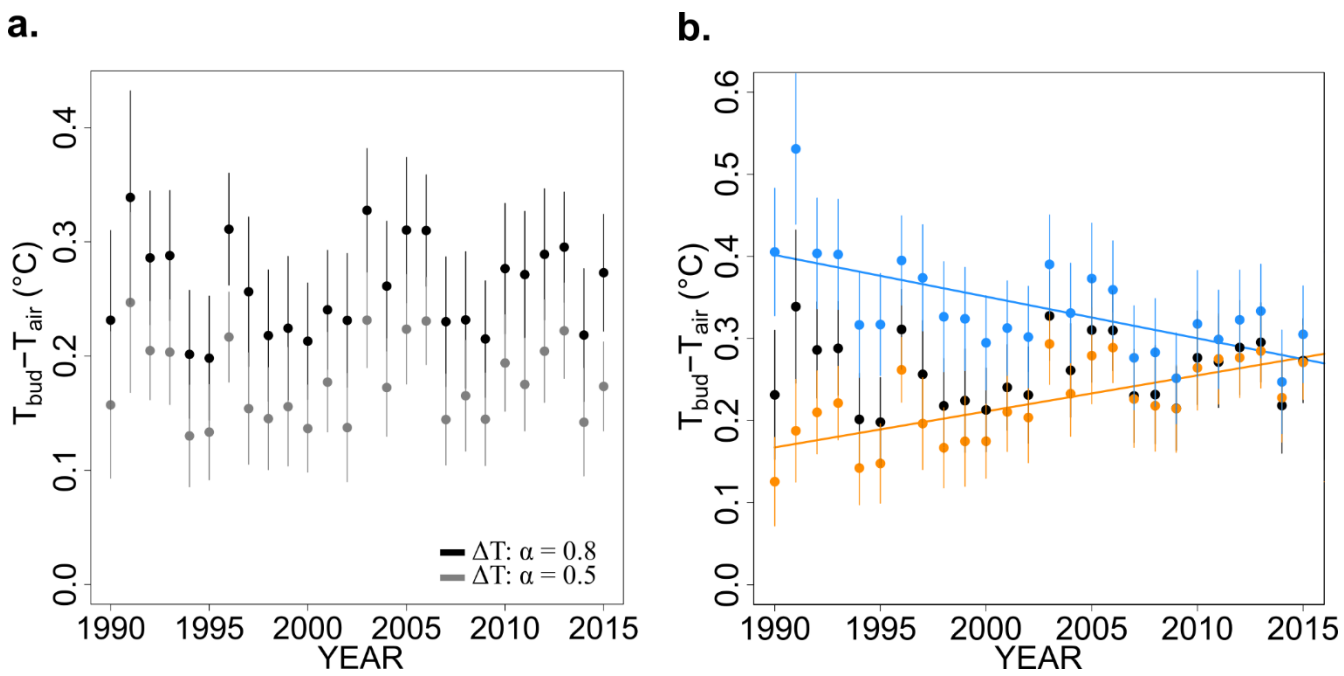

Figure 4 | Potential changes in T_{bud}-T_{air} over Europe. a. Each point corresponds to the mean preseason ΔTave (see Fig. 2) simulated for six deciduous species across Europe (1059 sites) under idealized conditions (i.e. sun-exposed buds) using field observation of budburst and global meteorological data (see Supplementary Material). All sites and species were pooled together. Two solar absorptivity values were tested, 0.5 (grey) and 0.8 (black). The error bars represent the spatial and species variability (±1 SD around the mean, n = 5050). **b.** Under these conditions, ΔT is expected to decrease (blue) over the period 1990-2015 (n = 375 sites*species, 7%) and increase (n = 670 sites*species, 13% in orange). The error bars represent the spatial and species variability (±1 SD around the mean). The black points correspond to all sites*species pooled together (n = 5050) with α = 0.8 as illustrated in panel a.

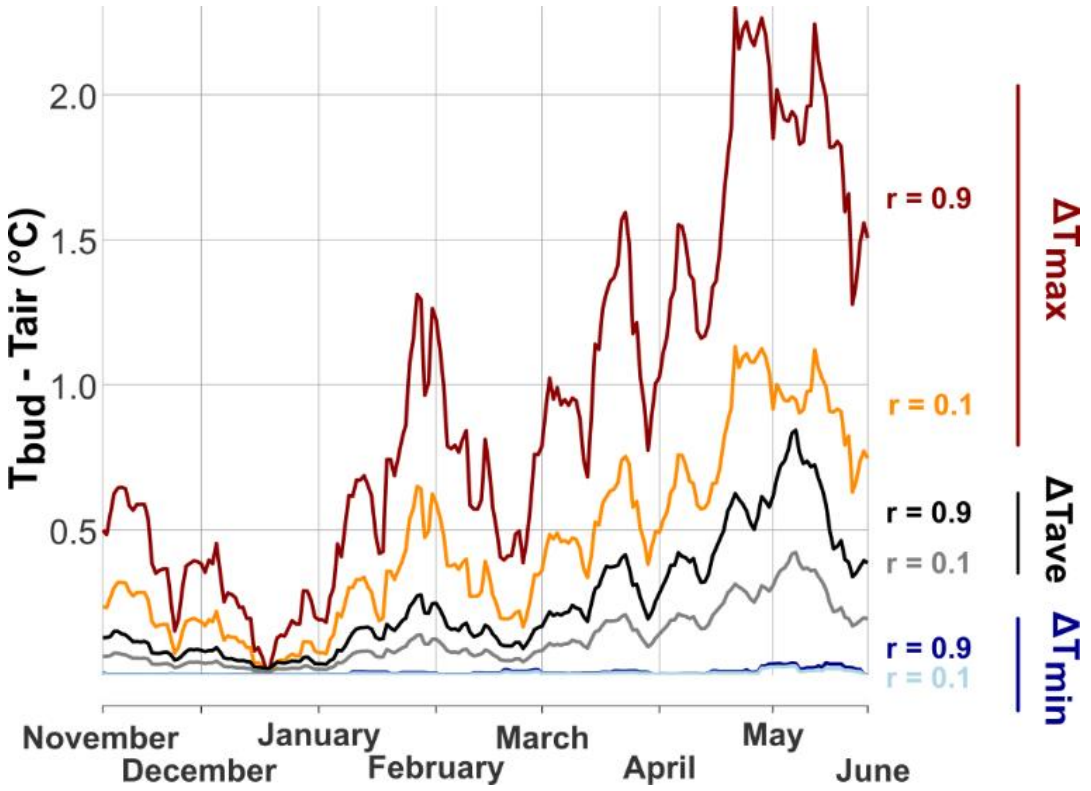

Figure 5 | Impact of ground albedo on simulated bud temperature. Temperature difference (ΔT in °C) between buds and air simulated for two different ground albedo, r = 0.1 (~wet bare soil) and r = 0.9 (~snow). Temperature difference was simulated using meteorological observations for winter and spring collected at the Hainich FLUXNET site (temperate deciduous forest, Germany; see Figure 2). The differences for maximum (red), average (black) and minimum (blue) temperatures are illustrated. Here, bud solar absorptivity to shortwave radiation and bud diameter were set to 0.8 and 5 mm, respectively

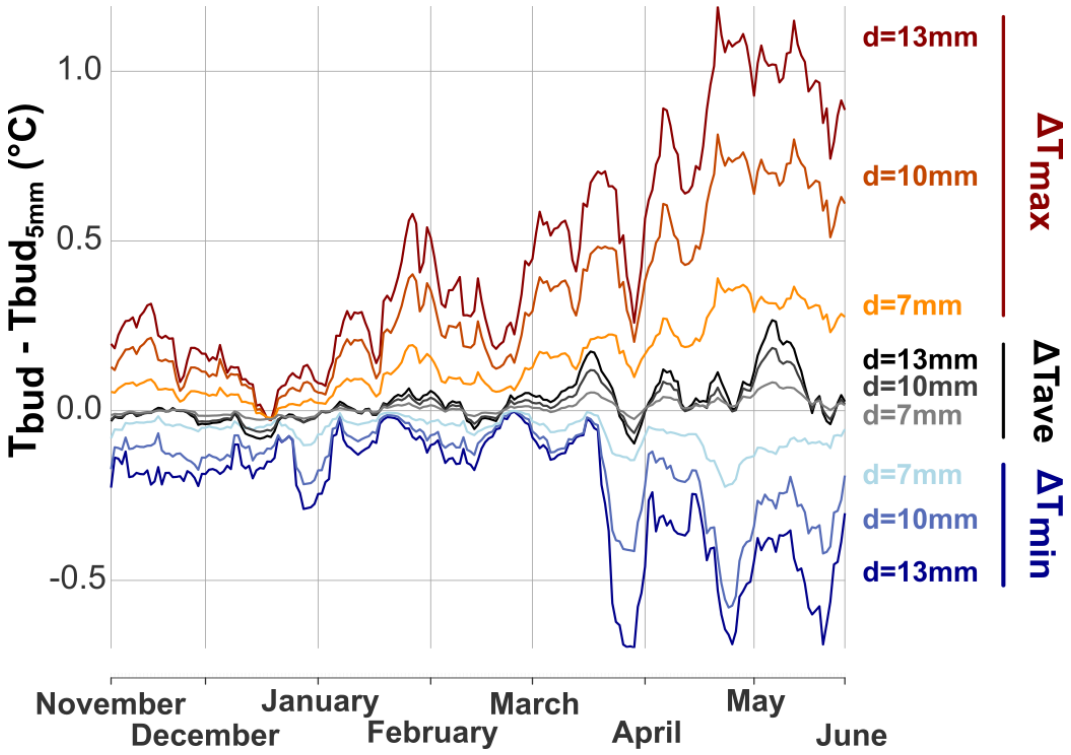

Figure 6 | Impact of bud size on simulated bud temperature. Temperature difference (ΔT in °C) between buds with a diameter (d) of 7, 10 and 13mm and buds with a diameter of 5mm. Temperatures were simulated using meteorological observations for winter and spring collected at the Hainich FLUXNET site (temperate deciduous forest, Germany; see Figure 2). The differences for maximum (red), average (black) and minimum (blue) temperatures are illustrated. Big buds exhibit larger temperature variations than small buds. Here, bud solar absorptivity to shortwave radiation and ground albedo were set to 0.8 and 0.2, respectively. Please note that these results represent the average change in bud temperature with a steady state model. With a low resolution of 30 min in meteorological forcing compared to the relatively small thermal time constant of buds, big buds have the time to accumulate more energy than small buds. Using a transient model, calibrated with site data and high-resolution micrometeorological observations accounting for the sudden changes in wind and radiation might lead to different results.

References

1. Peñuelas, J. & Filella, I. Phenology. Responses to a warming world. *Science (New York, N.Y.)* **294,** 793–795; 10.1126/science.1066860 (2001).
2. Peñuelas, J., Rutishauser, T. & Filella, I. Ecology. Phenology feedbacks on climate change. *Science (New York, N.Y.)* **324,** 887–888; 10.1126/science.1173004 (2009).
3. Ramos-Jiliberto, R., Moisset de Espanés, P., Franco-Cisterna, M., Petanidou, T. & Vázquez, D. P. Phenology determines the robustness of plant-pollinator networks. *Scientific reports* **8,** 14873; 10.1038/s41598-018-33265-6 (2018).
4. Chuine, I. Why does phenology drive species distribution? *Philosophical transactions of the Royal Society of London. Series B, Biological sciences* **365,** 3149–3160; 10.1098/rstb.2010.0142 (2010).
5. Chmielewski, F.-M. Phenology in Agriculture and Horticulture. In *Phenology: An Integrative Environmental Science,* edited by M. D. Schwartz. 2nd ed. (Springer Netherlands; Springer e-books; Imprint: Springer, Dordrecht, 2013), pp. 539–561.
6. Morellato, L. P. C. *et al.* Linking plant phenology to conservation biology. *Biological Conservation* **195,** 60–72; 10.1016/j.biocon.2015.12.033 (2016).
7. Katelaris, C. H. & Beggs, P. J. Climate change: allergens and allergic diseases. *Internal medicine journal* **48,** 129–134; 10.1111/imj.13699 (2018).
8. Schwartz, M. D. (ed.). *Phenology: An Integrative Environmental Science.* 2nd ed. (Springer Netherlands; Springer e-books; Imprint: Springer, Dordrecht, 2013).
9. Cleland, E. E., Chuine, I., Menzel, A., Mooney, H. A. & SCHWARTZ, M. D. Shifting plant phenology in response to global change. *Trends in ecology & evolution* **22,** 357–365; 10.1016/j.tree.2007.04.003 (2007).
10. Fu, Y. H. *et al.* Recent spring phenology shifts in western Central Europe based on multiscale observations. *Global Ecology and Biogeography* **23,** 1255–1263; 10.1111/geb.12210 (2014).
11. Jeong, S.-J., HO, C.-H., GIM, H.-J. & BROWN, M. E. Phenology shifts at start vs. end of growing season in temperate vegetation over the Northern Hemisphere for the period 1982-2008. *Global change biology* **17,** 2385–2399; 10.1111/j.1365-2486.2011.02397.x (2011).
12. Liu, Q. *et al.* Delayed autumn phenology in the Northern Hemisphere is related to change in both climate and spring phenology. *Global change biology* **22,** 3702–3711; 10.1111/gcb.13311 (2016).
13. Vitasse, Y. *et al.* Leaf phenology sensitivity to temperature in European trees: Do within-species populations exhibit similar responses? *Agricultural and Forest Meteorology* **149,** 735–744; 10.1016/j.agrformet.2008.10.019 (2009).
14. Wang, S. *et al.* Temporal Trends and Spatial Variability of Vegetation Phenology over the Northern Hemisphere during 1982-2012. *PloS one* **11,** e0157134; 10.1371/journal.pone.0157134 (2016).
15. Fu, Y. H. *et al.* Declining global warming effects on the phenology of spring leaf unfolding. *Nature* **526,** 104–107; 10.1038/nature15402 (2015).
16. Huang, M. *et al.* Velocity of change in vegetation productivity over northern high latitudes. *Nature ecology & evolution* **1,** 1649–1654; 10.1038/s41559-017-0328-y (2017).
17. Peaucelle, M. *et al.* Spatial variance of spring phenology in temperate deciduous forests is constrained by background climatic conditions. *Nature communications* **10,** 5388; 10.1038/s41467-019-13365-1 (2019).

18. Zohner, C. M., Mo, L., Pugh, T. A. M., Bastin, J.-F. & Crowther, T. W. Interactive climate factors restrict future increases in spring productivity of temperate and boreal trees. *Global change biology*; 10.1111/gcb.15098 (2020).

19. Montgomery, R. A., Rice, K. E., Stefanski, A., Rich, R. L. & Reich, P. B. Phenological responses of temperate and boreal trees to warming depend on ambient spring temperatures, leaf habit, and geographic range. *Proceedings of the National Academy of Sciences of the United States of America* **117,** 10397–10405; 10.1073/pnas.1917508117 (2020).

20. Zohner, C. M., Benito, B. M., Svenning, J.-C. & Renner, S. S. Day length unlikely to constrain climate-driven shifts in leaf-out times of northern woody plants. *Nature Clim Change* **6,** 1120–1123; 10.1038/nclimate3138 (2016).

21. Peñuelas, J. *et al.* Complex spatiotemporal phenological shifts as a response to rainfall changes. *New Phytologist* **161,** 837–846; 10.1111/j.1469-8137.2004.01003.x (2004).

22. Papagiannopoulou, C. *et al.* Vegetation anomalies caused by antecedent precipitation in most of the world. *Environ. Res. Lett.* **12,** 74016; 10.1088/1748-9326/aa7145 (2017).

23. Delpierre, N. *et al.* Modelling interannual and spatial variability of leaf senescence for three deciduous tree species in France. *Agricultural and Forest Meteorology* **149,** 938–948; 10.1016/j.agrformet.2008.11.014 (2009).

24. Fu, Y. H. *et al.* Nutrient availability alters the correlation between spring leaf-out and autumn leaf senescence dates. *Tree physiology* **39,** 1277–1284; 10.1093/treephys/tpz041 (2019).

25. Seyednasrollah, B., Swenson, J. J., Domec, J.-C. & Clark, J. S. Leaf phenology paradox: Why warming matters most where it is already warm. *Remote Sensing of Environment* **209,** 446–455; 10.1016/j.rse.2018.02.059 (2018).

26. Chuine, I., Morin, X. & Bugmann, H. Warming, photoperiods, and tree phenology. *Science (New York, N.Y.)* **329,** 277-8; author reply 278; 10.1126/science.329.5989.277-e (2010).

27. Vitasse, Y. & Basler, D. What role for photoperiod in the bud burst phenology of European beech. *Eur J Forest Res* **132,** 1–8; 10.1007/s10342-012-0661-2 (2013).

28. Way, D. A. & Montgomery, R. A. Photoperiod constraints on tree phenology, performance and migration in a warming world. *Plant, cell & environment* **38,** 1725–1736; 10.1111/pce.12431 (2015).

29. Caffarra, A., Donnelly, A. & Chuine, I. Modelling the timing of Betula pubescens budburst. II. Integrating complex effects of photoperiod into process-based models. *Clim. Res.* **46,** 159–170; 10.3354/cr00983 (2011).

30. Körner, C. & Basler, D. Plant science. Phenology under global warming. *Science (New York, N.Y.)* **327,** 1461–1462; 10.1126/science.1186473 (2010).

31. Fu, Y. H. *et al.* Daylength helps temperate deciduous trees to leaf-out at the optimal time. *Global change biology* **25,** 2410–2418; 10.1111/gcb.14633 (2019).

32. Singh, R. K., Svystun, T., AlDahmash, B., Jönsson, A. M. & Bhalerao, R. P. Photoperiod- and temperature-mediated control of phenology in trees - a molecular perspective. *New Phytologist* **213,** 511–524; 10.1111/nph.14346 (2017).

33. Flynn, D. F. B. & Wolkovich, E. M. Temperature and photoperiod drive spring phenology across all species in a temperate forest community. *New Phytologist* **219,** 1353–1362; 10.1111/nph.15232 (2018).

34. Brelsford, C. C., Nybakken, L., Kotilainen, T. K. & Robson, T. M. The influence of spectral composition on spring and autumn phenology in trees. *Tree physiology* **39,** 925–950; 10.1093/treephys/tpz026 (2019).

35. Strømme, C. B. *et al.* UV-B and temperature enhancement affect spring and autumn phenology in Populus tremula. *Plant, cell & environment* **38,** 867–877; 10.1111/pce.12338 (2015).

36. Fu, Y. H. *et al.* Increased heat requirement for leaf flushing in temperate woody species over 1980-2012: effects of chilling, precipitation and insolation. *Global change biology* **21,** 2687–2697; 10.1111/gcb.12863 (2015).

37. Huang, Y., Jiang, N., Shen, M. & Guo, L. Effect of preseason diurnal temperature range on the start of vegetation growing season in the Northern Hemisphere. *Ecological Indicators* **112,** 106161; 10.1016/j.ecolind.2020.106161 (2020).

38. Meng, F. *et al.* Opposite effects of winter day and night temperature changes on early phenophases. *Ecology* **100,** e02775; 10.1002/ecy.2775 (2019).

39. Zhang, S., Isabel, N., Huang, J.-G., Ren, H. & Rossi, S. Responses of bud-break phenology to daily-asymmetric warming: daytime warming intensifies the advancement of bud break. *International journal of biometeorology* **63,** 1631–1640; 10.1007/s00484-019-01776-0 (2019).

40. Meng, L. *et al.* Divergent responses of spring phenology to daytime and nighttime warming. *Agricultural and Forest Meteorology* **281,** 107832; 10.1016/j.agrformet.2019.107832 (2020).

41. Bigler, C. & Vitasse, Y. Daily Maximum Temperatures Induce Lagged Effects on Leaf Unfolding in Temperate Woody Species Across Large Elevational Gradients. *Frontiers in plant science* **10,** 398; 10.3389/fpls.2019.00398 (2019).

42. Fu, Y. H. *et al.* Three times greater weight of daytime than of night-time temperature on leaf unfolding phenology in temperate trees. *The New phytologist* **212,** 590–597; 10.1111/nph.14073 (2016).

43. Piao, S. *et al.* Leaf onset in the northern hemisphere triggered by daytime temperature. *Nature communications* **6,** 6911; 10.1038/ncomms7911 (2015).

44. Vitasse, Y. *et al.* Impact of microclimatic conditions and resource availability on spring and autumn phenology of temperate tree seedlings. *New Phytologist*; 10.1111/nph.17606 (2021).

45. Azeez, A. *et al.* EARLY BUD-BREAK 1 and EARLY BUD-BREAK 3 control resumption of poplar growth after winter dormancy. *Nature communications* **12,** 1123; 10.1038/s41467-021-21449-0 (2021).

46. HAMER, P. The heat balance of apple buds and blossoms. Part I. Heat transfer in the outdoor environment. *Agricultural and Forest Meteorology* **35,** 339–352; 10.1016/0168-1923(85)90094-2 (1985).

47. Landsberg, J. J., Butler, D. R. & Thorpe, M. R. Apple bud and blossom temperatures. *Journal of Horticultural Science* **49,** 227–239; 10.1080/00221589.1974.11514574 (1974).

48. Grace, J. The temperature of buds may be higher than you thought. *New Phytologist* **170,** 1–3; 10.1111/j.1469-8137.2006.01675.x (2006).

49. Muir, C. D. tealeaves: an R package for modelling leaf temperature using energy budgets. *AoB PLANTS* **11,** plz054; 10.1093/aobpla/plz054 (2019).

50. Jones, H. G. *Plants and microclimate. A quantitative approach to environmental plant physiology* (Cambridge university press, Cambridge, 2013).

554 51. Knohl, A., Schulze, E.-D., Kolle, O. & Buchmann, N. Large carbon uptake by an unmanaged 250-
555 year-old deciduous forest in Central Germany. *Agricultural and Forest Meteorology* **118,** 151–167;
556 10.1016/S0168-1923(03)00115-1 (2003).

557 52. Granier, A., Bréda, N., Longdoz, B., Gross, P. & Ngao, J. Ten years of fluxes and stand growth in a
558 young beech forest at Hesse, North-eastern France. *Ann. For. Sci.* **65,** 704; 10.1051/forest:2008052
559 (2008).

560 53. Zellweger, F. *et al.* Forest microclimate dynamics drive plant responses to warming. *Science (New*
561 *York, N.Y.)* **368,** 772–775; 10.1126/science.aba6880 (2020).

562 54. Bailey, B. N., Stoll, R., Pardyjak, E. R. & Miller, N. E. A new three-dimensional energy balance
563 model for complex plant canopy geometries: Model development and improved validation
564 strategies. *Agricultural and Forest Meteorology* **218-219,** 146–160;
565 10.1016/j.agrformet.2015.11.021 (2016).

566 55. Michaletz, S. T. & Johnson, E. A. A heat transfer model of crown scorch in forest fires. *Can. J. For.*
567 *Res.* **36,** 2839–2851; 10.1139/x06-158 (2006).

568 56. Sanchez-Lorenzo, A. *et al.* Reassessment and update of long-term trends in downward surface
569 shortwave radiation over Europe (1939–2012). *J. Geophys. Res. Atmos.* **120,** 9555–9569;
570 10.1002/2015JD023321 (2015).

571 57. Pfeifroth, U., Sanchez-Lorenzo, A., Manara, V., Trentmann, J. & Hollmann, R. Trends and
572 Variability of Surface Solar Radiation in Europe Based On Surface- and Satellite-Based Data
573 Records. *J. Geophys. Res. Atmos.* **123,** 1735–1754; 10.1002/2017JD027418 (2018).

574 58. Richardson, A. D. *et al.* Terrestrial biosphere models need better representation of vegetation
575 phenology: results from the North American Carbon Program Site Synthesis. *Glob Change Biol* **18,**
576 566–584; 10.1111/j.1365-2486.2011.02562.x (2012).

577 59. Liu, Q. *et al.* Extension of the growing season increases vegetation exposure to frost. *Nature*
578 *communications* **9,** 426; 10.1038/s41467-017-02690-y (2018).

579 60. Ma, Q., Huang, J.-G., Hänninen, H. & Berninger, F. Divergent trends in the risk of spring frost
580 damage to trees in Europe with recent warming. *Global change biology* **25,** 351–360;
581 10.1111/gcb.14479 (2019).

582 61. Zohner, C. M. *et al.* Late-spring frost risk between 1959 and 2017 decreased in North America but
583 increased in Europe and Asia. *Proceedings of the National Academy of Sciences of the United States*
584 *of America*; 10.1073/pnas.1920816117 (2020).

585 62. Xiao, L. *et al.* Estimating spring frost and its impact on yield across winter wheat in China.
586 *Agricultural and Forest Meteorology* **260-261,** 154–164; 10.1016/j.agrformet.2018.06.006 (2018).

587 63. Unterberger, C. *et al.* Spring frost risk for regional apple production under a warmer climate. *PloS*
588 *one* **13,** e0200201; 10.1371/journal.pone.0200201 (2018).

589 64. Leolini, L. *et al.* Late spring frost impacts on future grapevine distribution in Europe. *Field Crops*
590 *Research* **222,** 197–208; 10.1016/j.fcr.2017.11.018 (2018).

591 65. Greco, S. *et al.* Late Spring Frost in Mediterranean Beech Forests: Extended Crown Dieback and
592 Short-Term Effects on Moth Communities. *Forests* **9,** 388; 10.3390/f9070388 (2018).

593 66. Augspurger, C. K. Spring 2007 warmth and frost: phenology, damage and refoliation in a temperate
594 deciduous forest. *Functional Ecology* **23,** 1031–1039; 10.1111/j.1365-2435.2009.01587.x (2009).

67. Dong, N., Prentice, I. C., Harrison, S. P., Song, Q. H. & Zhang, Y. P. Biophysical homoeostasis of leaf temperature: A neglected process for vegetation and land-surface modelling. *Global Ecol Biogeogr* **26,** 998–1007; 10.1111/geb.12614 (2017).

68. University Of East Anglia Climatic Research Unit (CRU) & Harris, I. C. CRU JRA v1.1: A forcings dataset of gridded land surface blend of Climatic Research Unit (CRU) and Japanese reanalysis (JRA) data; Jan.1901 - Dec.2017, 2019.

69. Dupleix, A., Sousa Meneses, D. de, Hughes, M. & Marchal, R. Mid-infrared absorption properties of green wood. *Wood Sci Technol* **47,** 1231–1241; 10.1007/s00226-013-0572-5 (2013).

70. Howard, R. & Stull, R. IR Radiation from Trees to a Ski Run: A Case Study. *Journal of Applied Meteorology and Climatology* **52,** 1525–1539; 10.1175/JAMC-D-12-0222.1 (2013).

71. Monteith, J. L. & Unsworth, M. H. *Principles of environmental physics. Plants, animals, and the atmosphere.* 4th ed. (Elsevier/Academic Press, Amsterdam, Boston, 2013).

72. Bergman, T. L., Incropera, F. P. & Lavine, A. S. *Fundamentals of heat and mass transfer* (J. Wiley & Sons, Hoboken (N.J.), 2011).

73. Jacobs, A., Heusinkveld, B. G. & Kessel, G. Simulating of leaf wetness duration within a potato canopy. *NJAS - Wageningen Journal of Life Sciences* **53,** 151–166; 10.1016/S1573-5214(05)80003-X (2005).

74. Gerlein-Safdi, C. *et al.* Dew deposition suppresses transpiration and carbon uptake in leaves. *Agricultural and Forest Meteorology* **259,** 305–316; 10.1016/j.agrformet.2018.05.015 (2018).

75. Muñoz Sabater, J. Copernicus Climate Change Service: ERA5-Land hourly data from 1981 to present, 2019.

76. Kusch, E. & Davy, R. KrigR -- A tool for downloading and statistically downscaling climate reanalysis data, 04/06/2021.

77. R Core Team. *R: A Language and Environment for Statistical Computing*. Available at https://www.R-project.org/ (Vienna, Austria, 2018).